Noninflammatory 97-amino acid High Mobility Group Box 1 derived polypeptide disrupts and prevents diverse biofilms

Jaime D. Rhodes,[a] Aishwarya Devaraj,[a] Frank Robledo-Avila,[a] Sabarathnam Balu,[a] Lauren Mashburn-Warren,[a,b] John R. Buzzo,[a] Santiago Partida-Sanchez,[a,c] Lauren O. Bakaletz,[a,c,**] and Steven D. Goodman[a,c,*]

[a]Center for Microbial Pathogenesis, Abigail Wexner Research Institute at Nationwide Children's Hospital, Columbus, OH, 43205, USA
[b]The Steve and Cindy Rasmussen Institute for Genomic Medicine, Abigail Wexner Research Institute at Nationwide Children's Hospital, Columbus, OH, 43205, USA
[c]Department of Pediatrics, College of Medicine, The Ohio State University, Columbus, OH, 43210, USA

eBioMedicine
2024;107: 105304
Published Online xxx
https://doi.org/10.1016/j.ebiom.2024.105304

Summary

Background Bacterial biofilm communities are embedded in a protective extracellular matrix comprised of various components, with its' integrity largely owed to a 3-dimensional lattice of extracellular DNA (eDNA) interconnected by Holliday Junction (HJ)-like structures and stabilised by the ubiquitous eubacterial DNABII family of DNA-binding architectural proteins. We recently showed that the host innate immune effector High Mobility Group Box 1 (HMGB1) protein possesses extracellular anti-biofilm activity by destabilising these HJ-like structures, resulting in release of biofilm-resident bacteria into a vulnerable state. Herein, we showed that HMGB1's anti-biofilm activity was completely contained within a contiguous 97 amino acid region that retained DNA-binding activity, called 'mB Box-97'.

Methods We engineered a synthetic version of this 97-mer and introduced a single amino acid change which lacked any post-translational modifications, and tested its activity independently and in combination with a humanised monoclonal antibody that disrupts biofilms by the distinct mechanism of DNABII protein sequestration.

Findings mB Box-97 disrupted and prevented biofilms, including those formed by the ESKAPEE pathogens, and importantly reduced measurable proinflammatory activity normally associated with HMGB1 in a murine lung infection model.

Interpretation Herein, we discuss the value of targeting the ubiquitous eDNA-dependent matrix of biofilms via mB Box-97 used singly or in a dual host-augmenting/pathogen-targeted cocktail to resolve bacterial biofilm infections.

Funding This work was supported by NIH/NIDCD R01DC011818 to L.O.B. and S.D.G. and NIH/NIAID R01AI155501 to S.D.G.

Keywords: HMGB1; Inflammation; Humanised monoclonal antibody; *Burkholderia cenocepacia*; Bacterial infections

Introduction

High Mobility Group Box 1 (HMGB1) is a versatile host immune effector protein with multiple intra- and extracellular functions and is ubiquitous among eukaryotes. Intracellularly, HMGB1 functions as a DNA architectural element facilitating all manner of DNA transactions including replication, transcription, repair, and chromatin structure.[1–3] HMGB1 binds to and bends DNA with both high specificity and a particular affinity for bent DNA structures such as Holliday Junctions (HJs). Extracellularly, HMGB1 functions as a damage-associated molecular pattern (DAMP), a type of molecule that is released from impaired or dying cells to alert the host of cellular damage. As such, HMGB1 recruits polymorphonuclear neutrophils (PMNs), is additionally proinflammatory and both facilitates the induction of NETosis (the process by which PMNs release neutrophil extracellular traps or NETs) and is a component of NETs.[4] NETs are released as a part of the innate immune response to microbial infections; with the primary purpose of facilitating the killing of trapped individual microbes, and likely also to cordon off biofilm proliferation. During NETosis, PMNs are induced to release their own extracellular DNA (eDNA) with bound associated antimicrobial

*Corresponding author. 700 Children's Drive, WA5021, Columbus, OH, 43205, USA.
**Corresponding author. 700 Children's Drive, WA5009, Columbus, OH, 43205, USA.
E-mail addresses: Steven.Goodman@nationwidechildrens.org (S.D. Goodman), Lauren.Bakaletz@nationwidechildrens.org (L.O. Bakaletz).

Research in context

Evidence before this study

Novel strategies to resolve bacterial biofilm-mediated infections that tip the therapeutic balance in favor of the host are urgently needed, as these infections are notoriously recalcitrant to existing treatment approaches. We have shown that biofilm resistance to antibiotics and other modalities are attributable, in part, to the stability of an underlying bacterial extracellular DNA (eDNA) matrix, and that this matrix can be disrupted by the host innate immune effector HMGB1.

Added value of this study

We identified a 97 amino acid region of HMGB1 that fully retains anti-biofilm activity and engineered a synthetic version that is void of pro-inflammatory effects called 'mB Box-97_{syn}'. We demonstrated the 97-mer's heretofore unknown ability to disrupt biofilms and also prevent their formation in *in vitro* assays, as well as in murine models of both lung infection and endotoxemia without induction of excessive inflammation.

Implications of all the available evidence

mB Box-97_{syn} exhibits antibiofilm function against diverse pathogenic bacteria including the high priority ESKAPEE pathogens. The broad effectiveness of this peptide in the absence of demonstrable and potentially damaging excessive inflammation supports our continued development of a novel strategy to more effectively treat and resolve biofilm-mediated infections.

molecules (e.g., histones, cathelicidins, defensins).[5] These eDNA tendrils serve two purposes: to trap microbes and to concentrate the associated antimicrobial activity by both limiting diffusion and targeting bound antimicrobials to the entrapped pathogen, mechanisms by which PMN's sequester free living (planktonic) bacteria and thus protect the host. The existence of bacteria within biofilms, however, presents multiple challenges to normal PMN-mediated protective functions.

Biofilms are 3D communities of microorganisms that are either aggregated or adhered to a surface and exhibit differential gene expression to accommodate their multicellular community lifestyle. Importantly, bacteria within a biofilm produce a self-made matrix that, in part, protects the resident bacteria from environmental hazards that include host defenses and antimicrobials, while allowing free interaction amongst the resident bacteria. Indeed, biofilm-resident bacteria are typically 1000-fold or greater more tolerant of antibiotics than their isogenic counterparts that grow in planktonic form.[6] Importantly, biofilms are also resistant to PMN phagocytosis and NET-mediated clearance. Thus, when biofilms contribute to the pathogenesis of disease, these infections are extremely difficult to treat and resolve.

While there are species-specific substances that maintain the structural integrity of the biofilm matrix, it is eDNA that acts as a common infrastructural component. In fact, bacteria that are treated with DNase fail to form biofilms.[7,8] In contrast, however, as biofilms mature, their sensitivity to DNase wanes.[9,10] We showed that this latter resistance to the action of DNase is the result of a common eDNA lattice-like structure that generates fibers of DNA that are locked into the nuclease-resistant Z-form by HJ-like structures.[11] Importantly, these structures appear to be recapitulated in all biofilms assayed to date regardless of the constituent bacteria within the biofilm.[11] The commonality of this observation is owed to the fact that eDNA is a universal biofilm structural element. Moreover, all eubacteria express one or both members of the DNABII family of proteins: nucleoid-associated protein (HU) and integration host factor (IHF), which are integral to maintenance of the structural integrity of the eDNA-dependent biofilm matrix.[12] Intracellularly, the DNABII family, similar to eukaryotic HMGB1, acts as an architectural DNA element and is involved in all manner of DNA transactions within the prokaryotic cell. Previously, we and others showed that some of the intracellular DNABII family functions can be complemented by HMGB1.[13,14] Extracellularly, we showed that the DNABII family binds to and stabilises bent eDNA structures that functionally resemble HJs, which are essential to maintain structural integrity of the eDNA-dependent matrix of the biofilm[15]; however, sequestration of DNABII proteins from biofilms by high affinity antibodies disrupts these HJ-like structures.[15] As a consequence, the biofilm matrix collapses to release the resident bacteria regardless of the constituent resident species.[12,16–18]

We recently showed that the DNABII family of bacterial proteins and the eukaryotic HMGB1 protein, both of which are released at sites of infection, compete for the HJ-like structures within the eDNA lattice in the biofilm matrix.[14] However, unlike the bacterial DNABII proteins that stabilise the eDNA-dependent matrix to protect the resident bacteria, the host's HMGB1 protein de-stabilises this structure. Host prototypical endogenous levels of released HMGB1 appear to prevent biofilm proliferation by both interfering with biofilm structure and recruiting a strong innate immune response.[14,19] While this dual function serves to contain the resident bacteria in the biofilm without proliferation, it nonetheless fails to disrupt the biofilm nidus. Indeed, excessive native HMGB1 can cause sepsis,[20] likely due to the coupling of resident bacterial release from the biofilm and the recruitment of additional innate immune effectors. We showed that the uncoupling of these functions by inactivation of the proinflammatory functions, via mutagenesis of HMGB1, provides a powerful means to disrupt biofilms without negative inflammatory consequence.[14]

Antibodies directed against bacterial DNABII proteins work via sequestration of DNABII, whereas HMGB1 competitively inhibits DNABII binding to DNA. Both aforementioned strategies mediate a common outcome that is biofilm disruption, albeit by different mechanisms. As such, we previously showed compelling evidence for an advantageous effect of both approaches when used together in a cocktail. In an animal model of acute middle ear infection (otitis media) due to nontypeable *Haemophilus influenzae* (NTHI), anti-DNABII or an engineered modified version of recombinant HMGB1 (mHMGB1; characterised by a C45S point mutation to alleviate any undesired proinflammatory effects) each reduced the load of infectious bacteria in the middle ears of chinchillas by at least 5 logs, whereas use of the combination cocktail eliminated detectable bacteria in the middle ear by > 8 logs.[14]

In the new work presented here, we further characterised the recombinant HMGB1 (rHMGB1) protein to identify the antibiofilm portion of the molecule. We showed that complete antibiofilm activity was contained within a contiguous recombinant 97 amino acid peptide inclusive of one of three HMGB1 domains. In addition, we also modified this 97-mer peptide at a single amino acid (and was thus named 'mB Box-97') to alleviate its proinflammatory activity without loss of any effective antibiofilm activity *in vitro* or protective antibiofilm activity *in vivo*. Importantly, use of a synthetic version of mB Box-97 (mB Box-97_{syn}) demonstrated that there was no loss of antibiofilm activity, which strongly suggested that post translational modifications of this domain variant of HMGB1 were not critical for the observed anti-biofilm function. We also tested mB Box-97_{syn}'s ability to prevent biofilm formation by a panel of high priority bacterial pathogens. Finally, we tested this peptide in the presence or absence of a humanised anti-DNABII monoclonal antibody (HuTipMab) to determine if a cocktail of the peptide (engineered to augment host protective function) plus the monoclonal antibody (designed to target bacterial biofilms for disruption) were perhaps more effective at preventing biofilm formation than when either was used alone. Herein, we assessed whether the combination was a viable option for use as a therapeutic approach for treating and/or preventing biofilm-mediated infections. The potential effectiveness of this dual approach in improving medical management of pathogenic biofilms is discussed mechanistically and practically.

Methods

Humanised monoclonal antibody against a tip chimer peptide designed to mimic the immunoprotective domains of the DNABII protein integration host factor (IHF)

Humanised monoclonal antibody (of the IgG isotype) against the tip-chimer peptide (HuTipMab) was engineered from a murine monoclonal antibody and made for us under contract to Lake Pharma, Inc. (San Carlos, CA). Use of this antibody was validated by Western blot analysis, ELISA, and surface plasmon resonance with a Biacore 3000 instrument (GE Healthcare Life Sciences).[16]

Recombinant and synthetic proteins (Human rHMGB1, mHMGB1, HMGB1 A Box, B Box-87, mB Box-97_{rec}, A-B Boxes, 6His variants, mB Box-97_{syn})

N-terminal 6His-mB Box was cloned into pET-15b. Proteins were generated using the IMPACT kit (New England Biolabs). All constructs were confirmed by DNA sequencing. Proteins were purified to >95% purity using DEAE HiTrap and Heparin Sepharose columns and quantified using the Pierce BCA Protein Assay kit and SDS-PAGE with Coomassie Blue staining including known protein standards. Proteins were also confirmed by Western blot analysis (Supplementary Fig. S1). 97AA peptide mB Box-97_{syn} was synthesised (mB Box-97_{syn}; LifeTein®, LLC, Hillsborough, NJ) for ease of large-scale production and to > 95% homogeneity by HPLC.

Bacterial species and sources

NTHI strain 86-028NP was isolated from the nasopharynx of a child with chronic otitis media at Nationwide Children's Hospital.[21] UPEC strain UTI89 is a clinical isolate obtained from a person with cystitis.[22] *B. cenocepacia* strain K56-2 was isolated from a person with cystic fibrosis and obtained from Dr. Amal Amer.[23] *Enterobacter spp.* was isolated from a wound and obtained from Dr. Kelli Palmer.[24] *K. pneumoniae* was isolated from a pediatric urinary tract infection isolate.[25] *S. aureus* strain 29213 was isolated from a wound (obtained from the ATCC), *A. baumanii* strain 17978 was isolated from a fatal case of meningitis in a 4-month-old human (obtained from the ATCC) and *P. aeruginosa* strain 27853 was isolated from blood culture (obtained from the ATCC). *E. faecium* Com12 strain was isolated from feces of healthy human volunteers.[24] Strains not obtained from the ATCC were maintained frozen at low passage number in liquid nitrogen.

Disruption of bacterial biofilms

NTHI and *S. aureus* were cultured on chocolate agar for 18–24 h at 37 °C in a humidified atmosphere that contained 5% CO_2. NTHI was then resuspended in brain heart infusion broth supplemented with heme (2 μg/mL) and β-NAD (2 μg/mL) (sBHI) to an OD_{490} of 0.1. *S. aureus* was resuspended in brain heart infusion broth (BHI) to an OD_{490} of 0.1. The cultures were then diluted in their respective medium to contain approximately 2×10^5 CFU/mL, and 200 μL of this suspension was inoculated into each well of an 8-well chambered cover-glass slide (Thermo Fisher Scientific, Waltham, MA). *P. aeruginosa* and *E. faecium* were cultured on tryptic soy agar (TSA) as described above, then suspended in tryptic soy broth (TSB) to an OD_{490} of 0.1.

Cultures were then diluted in their respective medium as described above with 200 µL of this suspension used to inoculate each well of an 8-well chambered cover-glass slide. UPEC strain UT189, *B. cenocepacia, K. pneumoniae, Enterobacter sp.,* and *A. baumannii* were cultured on LB agar for 18–24 h at 37 °C in a humidified atmosphere that contained 5% CO_2. Cultures were then resuspended in LB as described above, and 200 µl of these suspensions were inoculated into each well of an 8-well chambered cover-glass slide. After 16 h of incubation of each bacterial species at 37 °C 5% CO_2, medium was replaced with the respective fresh medium and incubated for an additional 8 h. After a total incubation period of 24 h, medium was replaced with the respective fresh medium (control) or fresh medium that contained, A Box or (200 nM), B Box-87 (200 nM), A-B Box (200 nM), B Box-97 (200 nM), mB Box-97_{rec} (200 nM), mB Box-97_{syn} (200 nM), or HuTipMab (5.0 µg) and incubated at 37 °C 5% CO_2 for 2 h. All biofilms were then washed twice with 1 × Dulbecco's phosphate-buffered saline without calcium or magnesium (DPBS) (Corning, Corning, NY) and stained with LIVE/DEAD® stain (Thermo Fisher Scientific, Waltham, MA) per manufacturer's instructions. Biofilms were again washed then fixed with 1.6% paraformaldehyde, 0.025% glutaraldehyde, and 4% acetic acid in 0.1 M phosphate buffer at pH 7.4. Biofilms were imaged with a ×63 objective on a Zeiss 800 confocal laser scanning microscope (CLSM; Zeiss) wherein image selection was determined through analysis of the distribution of biofilm growth within chamber slide wells that best represented the entirety of each well, with areas in the proximity of where we introduced pipet tips and/or sides of chamber slide walls avoided. Images were analysed with COMSTAT2. Biomass values ($\mu m^3/\mu m^2$) were calculated by COMSTAT2 and represent the mean of 3 biological replicates that were repeated a minimum of three times on separate days ($n \geq 3$).

Analysis of A Box effect on NTHI and *S. aureus* biofilms

NTHI and *S. aureus* were cultured on chocolate agar for 18–24 h at 37 °C in a humidified atmosphere that contained 5% CO_2. NTHI was then resuspended in brain heart infusion broth supplemented with heme (2 µg/mL) and β-NAD (2 µg/mL) (sBHI) broth to an OD_{490} of 0.1. *S. aureus* was resuspended in brain heart infusion broth (BHI) to an OD_{490} of 0.1. The cultures were then diluted in their respective medium to contain approximately 2×10^5 CFU/mL, and 200 µL of this suspension was inoculated into each well of an 8-well chambered cover-glass slide (Thermo Fisher Scientific, Waltham, MA). After 24 h, biofilms were exposed to 400, 600, or 900 nM of A Box. After additional 2 h of incubation at 37 °C 5% CO_2, biofilms were washed once with DPBS then fixed, imaged, and analysed as described in previous *in vitro* assays.

Prevention of bacterial biofilm formation

NTHI and *S. aureus* were cultured and resuspended as described above then diluted in their respective medium to contain $\sim 5 \times 10^3$ CFU/mL or $\sim 1 \times 10^3$ CFU/mL, respectively, and 200 µL of this suspension was inoculated into each well of an 8-well chambered cover-glass slide. UPEC strain UTI89, *B. cenocepacia, K. pneumoniae, Enterobacter sp.*, and *A. baumanii* were cultured and resuspended as described above then diluted in LB broth to contain $\sim 1 \times 10^3$–1×10^5 CFU/mL, and 200 µL of this suspension was inoculated into each well of an 8-well chambered cover-glass slide. *P. aeruginosa* and *E. faecium* were cultured and suspended as described above then diluted to contain $\sim 1 \times 10^3$ CFU/mL, and 200 µL of this suspension was inoculated into each well of an 8-well chambered cover-glass slide. Upon incubation at 37 °C 5% CO_2 for 16h, rHMGB1 (200 nM), A Box (200 nM) mB Box-97_{rec} (600 nM), mB Box-97_{syn} (600 or 900 nM) or HuTipMab (5.0 or 7.5 µg) was added to respective wells containing each tested with the exception of media-only controls. Following 16 h incubation, all biofilms were washed once with DPBS and fixed as described above. Biofilms were imaged and analysed as described above. All assays represent the mean of 3 biological replicates that were repeated a minimum of three times on separate days ($n \geq 3$).

Determination of the efficacy of an mB Box-97_{syn} plus HuTipMab cocktail

NTHI and *S. aureus* were cultured on chocolate agar as described, then resuspended and diluted in their respective medium to contain $\sim 5 \times 10^3$ or $\sim 1 \times 10^3$ CFU/mL respectively, and 200 µL of this suspension was inoculated into each well of an 8-well chambered cover-glass slide. mB Box-97 and HuTipMab were added to these bacterial solutions to yield 56–900 nM and 0.5–7.5 µg, respectively, either in a cocktail or separately. After 13 h of incubation for *S. aureus* or 16 h of incubation for NTHI 37 °C 5% CO_2, biofilms were washed once with DPBS and fixed, imaged, and analysed as described in previous *in vitro* assays. Data represent the mean of 3 biological replicates that were repeated a minimum of three times on separate days ($n \geq 3$).

Intratracheal infection of *B. cenocepacia* in C57BL/6 mice

Female and male C57BL/6 mice were acquired from The Jackson Laboratory. Wildtype mice aged 10–14 weeks and approximately 20–25 g in body mass were used in all animal work presented herein. Mice were housed in BSL-2 facilities in individually ventilated cages at temperatures ranging from 20 to 24 °C with filtered air, and a 12 h light/12 h dark cycle. Absorbing bedding, drinking water, and a standardised mouse diet was provided, and all materials were autoclaved before use. CFU in lungs were quantified from four to five mice per group, and lung pathology was analysed from

two mice per group, which while not able to provide a statistical comparison was nonetheless informative. *B. cenocepacia* strain K56-2 was cultured in Luria–Bertani (LB) broth (Difco, MD) at 37 °C overnight with shaking. Bacterial concentration was adjusted before each experiment based on absorbance at 600 nm. Mice were treated with 2 μg of B Box-97 or mB Box-97$_{syn}$ peptides contained within a 100 μl volume at the time of bacterial challenge. Animals were euthanised 72 h post infection for recovery of bronchoalveolar lavage (BAL) fluids and lungs for homogenisation. The number of CFU of bacteria in both BAL fluids and lung tissue homogenates was calculated by performing serial dilutions and seeding aliquots onto LB agar plates. Lungs were also fixed and embedded in paraffin; slides were stained with Hematoxylin-Eosin (H&E) and relative evidence of histopathology and/or inflammation was assessed.

Murine model of endotoxemia

C57BL/6 mice were acquired and housed according to the methodology described above. Male and female mice in groups of three to five were injected IP with either PBS, 100 μg of *E. coli* Lipopolysaccharides (LPS) (Sigma), 2 μg endotoxin-free B Box-97, or 2 μg endotoxin-free mB Box-97$_{syn}$. The size per group was not calculated based on statistic methods. Mice were euthanised 24 h later, serum was collected and relative concentration of TNF-α was quantified by ELISA (Thermo Fisher). Our study examined male and female animals, and similar findings are reported for both sexes.

Ethics

All animal experiments were performed in compliance with established ethical regulations and approved by the Institutional Animal Care and Use Committee (IACUC) at NCH (Nationwide Children's Hospital) according to protocol AR13-00020, in which the methodology is described in detail.

Statistics

Graphical results were analysed, and statistical tests were performed with GraphPad Prism 9 for all *in vitro* assays. Due to the small sample sizes used throughout the manuscript, a Shapiro–Wilk test for normality was performed on all data as well as a nonparametric Kruskal–Wallis test (with an uncorrected Dunn's test for multiple comparisons) to ensure that any stated statistical significance with parametric one-way ANOVAs (with Dunnett's multiple comparison correction) (or lack thereof) were retained. Results from parametric testing are retained when data were normally distributed, and non-parametric test outcomes are reported for data that were not normally distributed. Data are presented as mean ± SEM and significance is shown as *P ≤ 0.05, **P < 0.01, ***P < 0.001, and ****P < 0.0001. *n* represents the number of biological replicates and is defined within respective figure legends.

Role of funders

Funders did not participate in the study design, data collection, data analyses, interpretation, or writing of the manuscript. The corresponding authors had full access to all of the data and had the final responsibility to submit for publication.

Results

Domain structure of HMGB1 and rationale for generation of truncated constructs

HMGB1, produced exclusively by eukaryotes, is >99% conserved amongst mammals as a chromatin component.[26] HMGB1 acts as a monomer and consists of two structurally similar but distinct alpha helical-containing domains that bind to and bend DNA (A and B Boxes), plus a third C terminal domain comprised of ~30 consecutive acidic residues that interacts with a wide variety of protein partners in chromatin (Fig. 1). To engineer a therapeutic version of HMGB1 that solely functions to disrupt bacterial biofilms whilst void of pro-inflammatory activity, we sought to identify the specific minimum region(s) of the native protein that possess antibiofilm ability only. To do so, we produced rHMGB1 truncated variants that included: 1) an A-B Boxes construct (lacks the C tail; residues 1–176); 2) the A Box, a self-contained DNA-binding domain[27] (AA residues 1–89); 3) an 87 residue portion that contained the B Box ('B Box-87', residues 90–176); and 4), and a 97 residue portion that contained an extended version of the B Box ('B Box 97', residues 80–176) (Fig. 1). Previous work implied DNA binding was required for anti-biofilm function, and regions directly adjacent to the B-Box

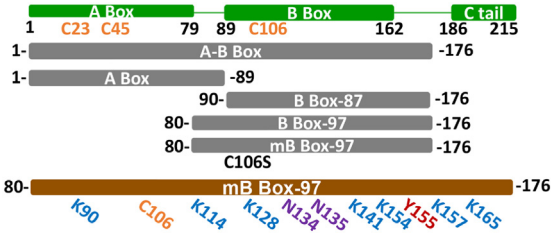

***Fig. 1:* Structure of HMGB1.** Domain structure of HMGB1 (green). The amino acids (AAs) for each domain are indicated (black), and cysteine residues C23 and C45 can form a disulfide bond that results in reduced DNA binding affinity and increased pro-inflammatory activity. C106 mediates pro-inflammatory activity via TLR4-MD2 binding. Engineered HMGB1 domain variants are shown (gray). Multiple AAs in mB Box-97 can be post-translationally modified (PTM) [brown bar shows points of PTM: acetylation/methylation of Lys (blue); oxidation of Cys (orange); glycosylation of Asn (purple); phosphorylation of Tyr (red)].

(linkers) contain additional DNA binding activity.[28] As the B Box is reported to contain pro-inflammatory activity, mediated primarily through interactions with TLR4-MD2 that are dependent through residue C106,[29] we created a modified recombinant B Box-97 variant (mB Box-97_{rec}) with a C106S mutation.

B Box-containing HMGB1-derived peptides retained *in vitro* biofilm disruption activity

First, we tested disruptive abilities of rHMGB1-derived peptides. These peptides were evaluated for their ability to disrupt established biofilms (formed for 24 h prior to addition of an HMGB1 variant). After a 16 h exposure to a single dose of each peptide (200 nM), biofilms formed by a variety of high priority pathogens were stained with LIVE/DEAD®, imaged by confocal laser scanning microscopy (CLSM), analysed by COMSTAT,[30] and compared to biofilms incubated with media only (negative control). Addition of A Box (200 nM) to established biofilms formed by uropathogenic *Escherichia coli* (UPEC), *Burkholderia cenocepacia* (*Bc*), *Klebsiella pneumoniae* (*Kp*) or nontypeable *Haemophilus influenzae* (NTHI) had no significant effect on measured biofilm thickness when analyzed by either parametric or nonparametric one-way analysis of variance (ANOVA; corrected for multiple comparisons with Dunnet's tests or uncorrected Dunn's test of multiple comparisons, respectively) and in some cases appeared to slightly stimulate biofilm growth over that of exposure to medium alone (Fig. 2A). While B Box-87 exhibited significant anti-biofilm activity against *B. cenocepacia, K. pneumoniae* and NTHI (but had no measurable effect on UPEC biofilms) when analyzed with parametric one-way ANOVA compared to media alone, nonparametric ANOVA results of these data suggest that significance was not retained when B Box-87 was tested against NTHI (although these data are normally distributed as indicated by a Shapiro–Wilk test for normality; due to relatively small sample size, we ran these additional nonparametric tests to account for this limitation and ensure a comprehensive analysis of this exploratory study in order to confirm the effectiveness of mB Box-97 as compared to other peptides for use in future studies). A-B Box and B Box-97 peptides retained highly significant anti-biofilm activity against all pathogens tested when analyzed by both parametric and non-parametric one-way ANOVA ($P = 0.004$–$P < 0.0001$; with the exception of A-B Box tested against NTHI, which; although normally distributed and statistically significant by parametric one-way ANOVA, approaches significance ($P = 0.055$) when analyzed by nonparametric one-way ANOVA)) (Fig. 2A). Modified B-Box variant mB Box-97_{rec} also significantly disrupted biofilms formed by all pathogens tested ($P = 0.0025$–$P < 0.0001$) as indicated by both parametric and nonparametric one-way ANOVA results (Fig. 2A).

Native HMGB1 is heavily post translationally modified, which affects various HMGB1 functions.[31] Indeed, even recombinant proteins expressed by bacteria often have post translational modifications. Thus, we synthesised a 97 amino acid peptide based on the coding sequence of mB Box-97_{rec}, which will henceforth be referred to as mB Box-97_{syn}. mB Box-97_{syn} significantly disrupted biofilms formed by four additional high priority ESKAPEE pathogens: *Pseudomonas aeruginosa* (*Pa*), *Staphylococcus aureus* (*Sa*), *Enterococcus faecium* (*Ef*), and *Acinetobacter baumannii* (*Ab*) (Fig. 2B). In these assays, we also integrated use of a humanised monoclonal antibody directed against the binding tips of the bacterial DNABII proteins ('HuTipMab'), previously shown to have broad biofilm disruption activity[16] as a positive control (Fig. 2B). Biofilms formed for 24 h prior to the addition of media alone, A Box (200 nM), mB Box-97_{syn} (200 nM) or HuTipMab (5.0 μg; equivalent to a concentration of 342 nM). After a 2 h exposure to a single dose of each treatment, biofilms were imaged and analysed as described above for Fig. 2A, and average percent biomass remaining was reported. Each pathogen was significantly disrupted by mB Box-97_{syn} or HuTipMab (*Pa*–70%, 70%; *Sa*–88%, 75%; *Ef*–61%, 71%; *Ab*–83%, 72%, respectively) ($P = 0.03$–$P < 0.0001$) compared to treatment with media only (negative control). At 200 nM, A Box again appeared to stimulate growth of both *P. aeruginosa* and *E. faecium* biofilms over that of incubation with medium alone.

To ensure that mB Box-97_{syn} retained its ability to act as a biofilm disruptive agent against even larger and/or older biofilms, we tested the ability of the peptide to disrupt those formed by the respiratory tract pathogen NTHI. To this end, biofilms grown for 48 or 72 h were exposed to a single dose of mB Box-97_{syn} (200 nM) for an additional 2 h, then imaged and analysed as described in aforementioned *in vitro* biofilm disruption assays. As a positive control for this assay we exposed replicate NTHI biofilms to a murine monoclonal antibody (MsTipMab is directed against the same protective epitopes as is HuTipMab; used at 5.0 μg) or, as a negative control, to a murine monoclonal antibody directed against a non-protective domain of a bacterial DNABII protein (MsTailMab; 5.0 μg). Whereas, compared to incubation with media alone, neither 48 nor 72 h NTHI biofilms were disrupted by incubation with MsTailMab, they were significantly disrupted by both MsTipMab and mB Box-97_{syn} (48 h: 47% and 47%; 72 h: 34% and 46%, respectively) (Supplementary Fig. S2) ($P = 0.0007$–$P < 0.0001$). Biofilms grown for 96 h required twice the aforementioned concentrations of MsTipMab or mB Box-97_{syn} (10.0 μg or 400 nM, respectively) to elicit similar disruption (e.g., 37% and 49%, respectively). The need for an increased dose of therapeutic was expected, given that eDNA and DNABII concentrations increase with biofilm maturity.[11] These

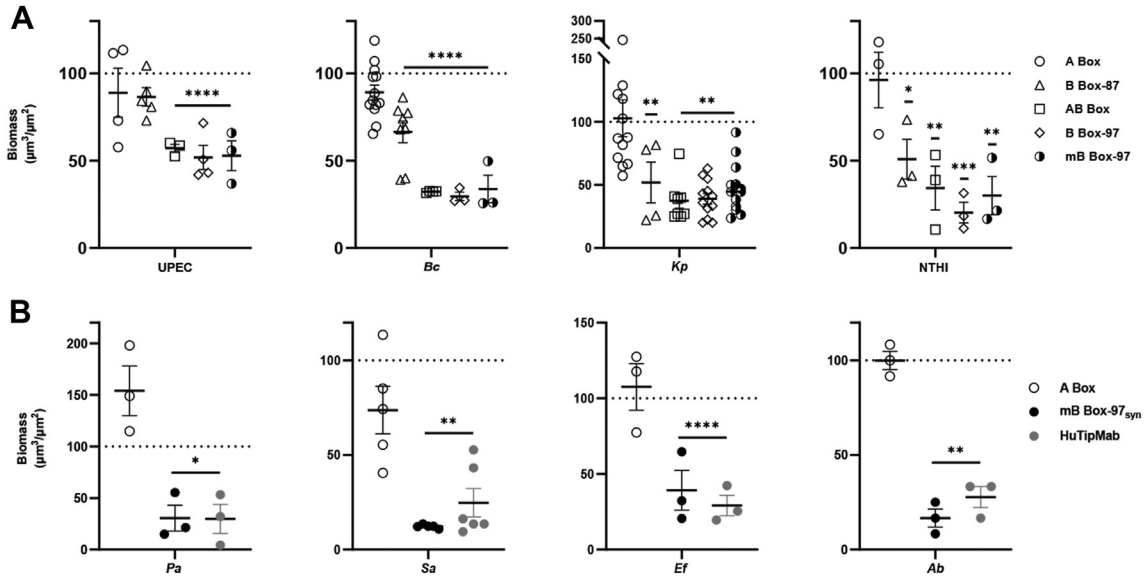

Fig. 2: **Disruption of biofilms formed by ESKAPEE pathogens, NTHI, or *B. cenocepacia*.** (**A**) Individual domains of rHMGB1 (200 nM) were added at 24 h to the respective preformed biofilms, *in vitro*, for 16 h. Biofilms were stained with LIVE/DEAD®, imaged by confocal laser scanning microscopy (CLSM), and analysed by COMSTAT to calculate average thickness and comparison to media alone control was plotted (dotted line indicates control values). Data presented are mean ± SEM. Statistical significance compared to control was assessed with one-way ANOVA (*P < 0.05, **P < 0.01, ***P < 0.001, and ****P < 0.0001). (**B**) A Box (200 nM), mB Box-97_{syn} (200 nM), or HuTipMab (5.0 µg) were added at 24 h to biofilms pre-formed by additional ESKAPEE pathogens, *in vitro*, for an additional 2 h. Biofilms were stained with LIVE/DEAD®, imaged as described in **2A**, and analysed by COMSTAT to calculate average biomass and percent biomass remaining compared to the media only control was plotted (dotted line indicates control values). Treatment groups represent a minimum of n = 3.

results were statistically significant (P = 0.02, P = 0.004, respectively).

mB Box-97_{syn} retains DNA binding function and is stable *in vitro*

To further determine if post-translational modifications played a role in biofilm disruption, mB Box-97_{rec}, was compared to mB Box-97_{syn}, and used to confirm that it indeed retained DNA binding activity. We performed an electromobility shift assay (EMSA) using a HJ DNA substrate that mimics the crossed strands of the eDNA lattice of bacterial biofilms[15] and is also a natural substrate of HMGB1[14] and compared the binding ability of mB Box-97_{syn} to that of the various truncations of HMGB1. Recombinant versions of all truncations that contained complete A and or B Box domain structures including mB Box-97_{rec} and mB Box-97_{syn} were similarly able to bind to HJ DNA (Supplementary Figs. S3 & S4). As an additional test of stability, mB Box-97_{syn} was incubated in human serum and shown to be stable for a minimum of 24 h (Supplementary Fig. S5), consistent with the fact that both the construct structure and a lack of post translational modifications of mB Box-97_{syn} failed to affect protein stability. Collectively these data suggested that mB Box97_{syn} (which lacked any post-translational modifications) maintained both the DNA-binding and biofilm disrupting capabilities of mB Box97_{rec}, and further, was stable in human serum. Lastly, we conducted a series of growth curve determinations to confirm that neither B Box-97 or mB Box-97_{syn} (when assayed at the concentrations used for anti-biofilm activity) exhibited any bactericidal activity (Supplementary Fig. S6) and saw no change in the growth rate of NTHI.

mB Box-97_{syn} prevented biofilm formation *in vitro*

We hypothesised that mB Box-97_{syn} could also prevent the formation of bacterial biofilms, as this hypothesis is consistent with the domain variant's now demonstrated ability to disrupt established biofilms *in vitro*. To this end, we assayed for the ability of mB Box-97_{syn} to prevent biofilm formation by *S. aureus* or NTHI, a representative Gram-positive or Gram-negative pathogen, respectively. Negative controls included exposure to media alone or to A Box (200 nM) given its demonstrated lack of biofilm disruption activity and tendency to slightly stimulate biofilm growth even when used at up to 900 nM when incubated with either of these bacterial pathogens. Established biofilms treated with A Box after an initial incubation period (24 h) then assayed for relative disruption are presented in Fig. 3. To assay biofilm prevention capability, inocula were exposed to either whole rHMGB1 (200 nM), mB Box-97_{rec} (600 nM) or two concentrations of mB Box-97_{syn}

(600 or 900 nM). We used greater concentrations of these latter agents (e.g., 600 or 900 nM) as biofilm prevention required an increased concentration over that used for disruption (data not shown). Due to what is known regarding its biofilm disruption capability, we also tested, for the first time, HuTipMab's ability to prevent biofilm formation via use of two increasing concentrations of (5.0 or 7.5 μg), for 16 h. Biofilms were then stained with LIVE/DEAD®, imaged by CLSM then analysed by COMSTAT. Average biofilm biomass values compared to those when incubated with media alone were used to report percent prevention.

Neither exposure to media alone nor A Box prevented growth of *S. aureus* or NTHI biofilms, and as noted earlier, exposure to 200 nM of A Box appeared to slightly stimulate *S. aureus* biofilm growth over that of exposure to medium alone. Conversely however, growth of both *S. aureus* and NTHI biofilms was significantly prevented by exposure to mB Box-97_{syn} or HuTipMab at each concentration tested compared to both negative controls (Fig. 4A) ($P = 0.01–P<0.0001$). The highest tested concentrations of mB Box-97_{syn} and HuTipMab (e.g., 900 nM and 7.5 μg, respectively) prevented growth beyond that of a monolayer of bacteria (average biomass $<1.0\ \mu m^3/\mu m^2$, $P < 0.0001$), characterised by the absence of characteristic biofilm 3D architecture. Additionally, rHMGB1 and mB Box-97_{rec} were similarly preventative ($P = 0.009–P = 0.0001$) which indicated that the full anti-biofilm activity of both recombinant proteins was maintained within mB Box-97_{syn} which lacked post-translational modifications.

To determine the breadth of ability of mB Box-97_{syn} and now established positive control HuTipMab to prevent biofilm formation by additional human pathogens, we used the most effective concentration of each biological that had prevented biofilm formation by both *S. aureus* and NTHI to attempt to similarly prevent biofilm formation by the remaining high priority ESKAPEE pathogens or *Burkholderia cenocepacia* (Fig. 4B). Whereas exposure to A Box or media alone again did not prevent biofilm growth by any pathogen tested, and at times once again appeared to slightly stimulate growth compared to exposure to medium alone (e.g., UPEC, *B. cenocepacia*), we observed significant prevention of biofilm formation by *P. aeruginosa*, *Enterobacter spp.*, *E. faecium*, UPEC, *A. baumannii* or *B. cenocepacia* after 16h exposure to either mB Box-97_{syn} or HuTipMab, as indicated by reported average remaining biomass values. To provide additional evidence of the preventative activity observed, data generated with the pathogen *K. pneumoniae* (Fig. 5A) are presented along with corresponding representative CLSM images and average remaining biomasses are reported, with A Box again slightly stimulating *K. pneumoniae* biofilm growth over that of medium alone (Fig. 5B). Biomass differences of every pathogen tested compared to respective media alone or to A Box exposures were statistically significant ($P = 0.04–P < 0.0001$), with the exception of *K. pneumoniae*, which approaches significance ($P = 0.055$) when mB Box-97_{syn} was compared to media alone or A Box.

An mB Box-97_{syn} and HuTipMab cocktail was more effective at prevention of biofilm formation than either agent when used separately

As we had demonstrated to this point that exposure to either mB Box-97_{syn} or HuTipMab significantly prevented biofilm formation by 9 pathogens including the 7 high priority ESKAPEEs *in vitro*, we hypothesised that the two modalities would yield an even greater preventive effect when utilised simultaneously, given that they function via different yet potentially complementary

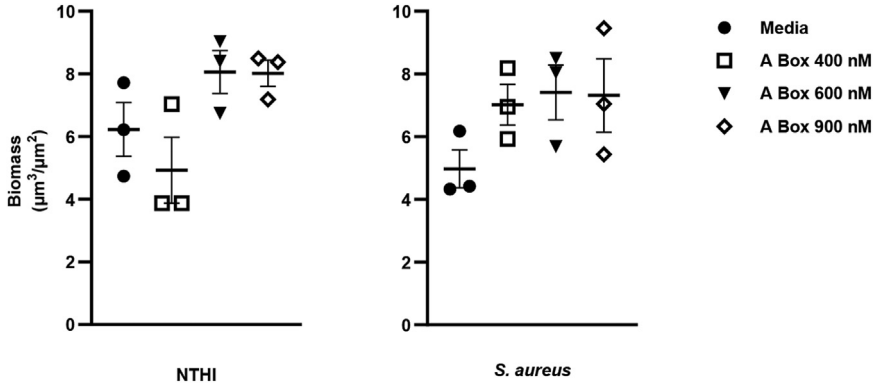

Fig. 3: **HMGB1-derived A box peptide did not disrupt NTHI or *S. aureus* biofilms** Incubation with HMGB1-derived A Box peptide did not disrupt biofilms formed by either NTHI or *S. aureus* at any of the tested concentrations. Each biofilm was allowed to grow for 24 h, then incubated for an additional 2 h with one of three increasing concentrations of A Box. Use of 400 nM A Box again appeared to slightly stimulate growth of *S. aureus* biofilms, whereas incubation with either 600 or 900 nM of A Box slightly stimulated growth of biofilms formed by both pathogens. Data are presented as mean ± SEM. Statistical significance compared to control was assessed with one-way ANOVA and no comparisons were significant (*$P < 0.05$). Treatment groups represent n = 3.

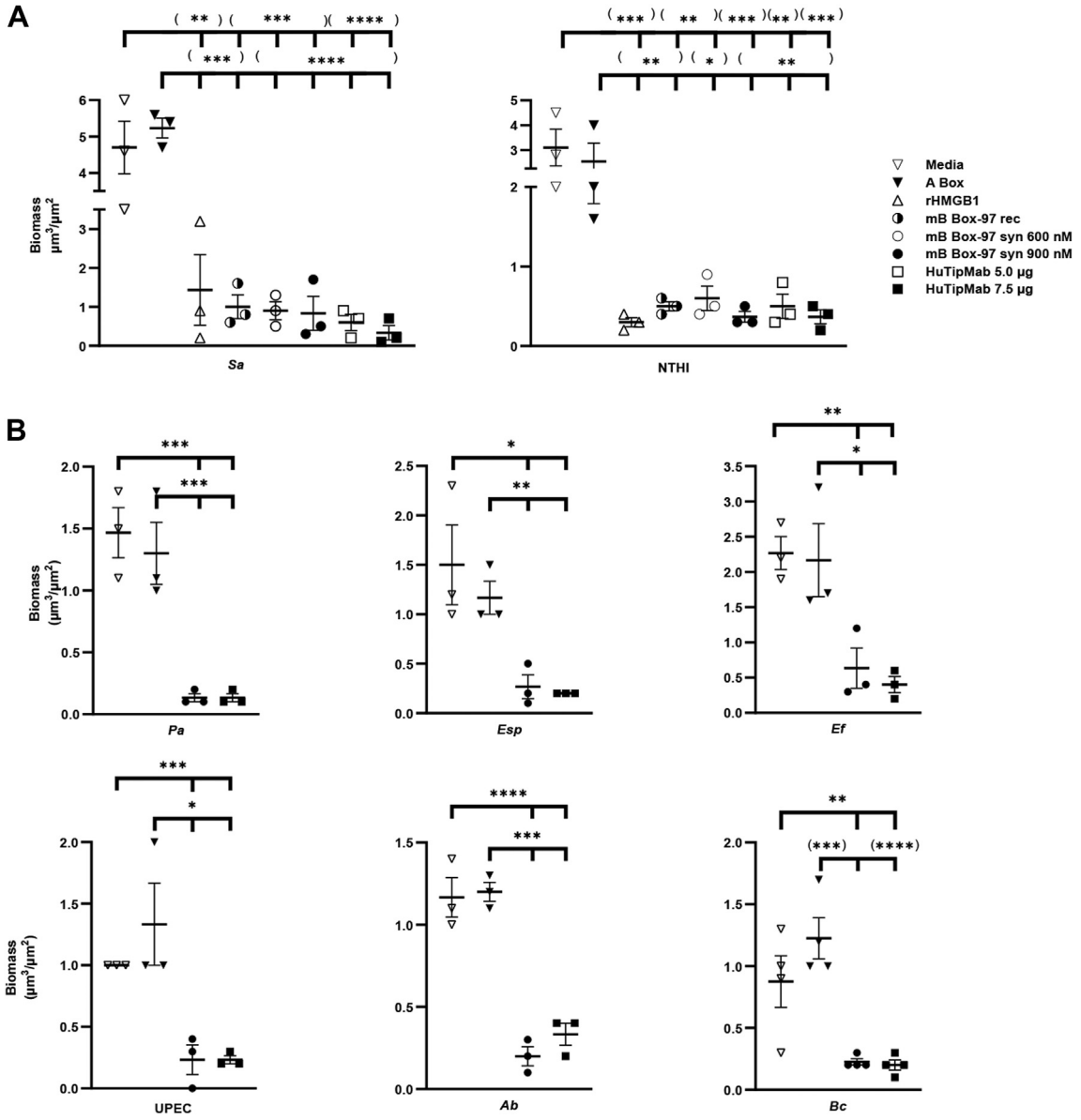

Fig. 4: **Prevention of biofilm formation by ESKAPEE pathogens, NTHI or *B. cenocepacia*.** (**A**) *S. aureus* or NTHI exposed to media alone or single dose concentrations of A Box (200 nM), rHMGB1 (200 nM), mB Box-97_{rec} (600 nM), mB Box-97_{syn} (600 or 900 nM) or HuTipMab (5.0 or 7.5 µg), for 16 h. Biofilms were stained with LIVE/DEAD®, imaged by CLSM, analysed by COMSTAT, and average biomass remaining compared to media alone or A Box was plotted. Data presented are mean ± SEM. Statistical significance compared to control was assessed with one-way ANOVA (*P < 0.05, **P < 0.01, ***P < 0.001, and ****P < 0.0001). (**B**) *P. aeruginosa, E. species, E. faecium,* UPEC, *A. baumannii, or B. cenocepacia* exposed to media alone or single dose concentrations of A Box (200 nM), mB Box-97_{syn} (900 nM) or HuTipMab (7.5 µg), for 16 h. Biofilms were stained, imaged, analysed and data are presented as described in **4A**. What appears to be identical media biomass measurements for UPEC biofilms represent raw values of 0.96, 1.01, and 0.97 $\mu m^3/\mu m^2$ which were each rounded to 1.0 and reflect UPEC's consistent growth at the tested inoculum and incubation period.

mechanisms. To establish a comparative model that evaluated preventative effects of each agent separately alongside that of an admixed cocktail, we exposed a representative Gram positive or Gram negative pathogen (e.g., *S. aureus* or NTHI) to serial 1:2 dilutions of a starting maximal dose of either mB Box-97_{syn} or HuTipMab (see Key portion of Table 1 below the dotted line) used in earlier prevention assays as compared to exposure to media alone to determine relative preventative capabilities.

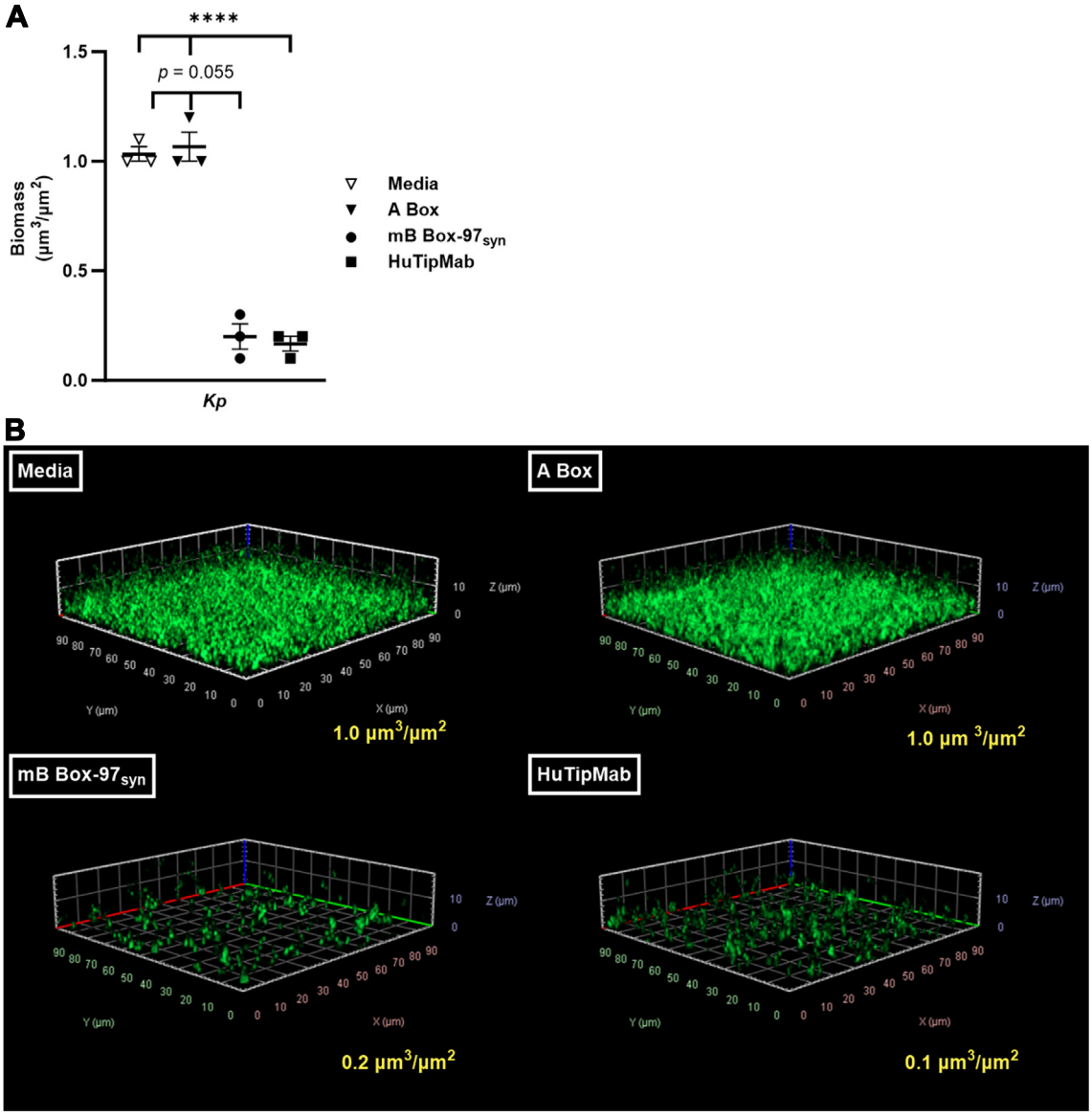

Fig. 5: **Prevention of biofilm formation by *K. pneumoniae*.** (**A**) *K. pneumoniae* exposed to single dose concentrations of media alone, A Box (200 nM), mB Box-97_{syn} (900 nM), or HuTipMab (7.5 μg) for 16 h. Biofilms were stained with LIVE/DEAD®, imaged by CLSM, analysed by COMSTAT, and average biomass remaining compared to media alone or A Box was plotted. Data presented are mean ± SEM. Statistical significance compared to control was assessed with one-way ANOVA ($P \leq 0.05$, ****$P < 0.0001$). (**B**) Representative CLSM images of LIVE/DEAD® stained *K. pneumoniae* biofilms from data shown and described above.

As shown, a 13 h exposure to decreasing concentrations of mB Box-97_{syn} (top row, Table 1A) prevented *S. aureus* biofilm formation from 79% to 0%, whereas a 13 h exposure to decreasing concentrations of HuTipMab (second row, Table 1B) prevented *S. aureus* biofilm formation from 82% to 0%. Following a 16 h exposure to decreasing concentrations of mB Box-97_{syn} (top row, Table 1B), biofilm formation of NTHI was prevented from 62% to 0% whereas following the same exposure to and dilutions of HuTipMab (second row, Table 1B), biofilm formation of NTHI was prevented from 67% to 0%. Exposure of *S. aureus* or NTHI to decreasing concentrations of a 1:1 cocktail of both biologicals (mB Box-97_{syn} plus HuTipMab) for 13–16 h was also tested (see values within the bottommost row associated with each pathogen in Table 1). Percent prevention of *S. aureus* (Panel A, bottommost row), following exposure to the admixed cocktail ranged from 92% to 0% which exceeded that of either biological when used alone at every concentration tested, except for the lowest tested

A. *S. aureus*						
mB Box-97	79 ± 5	65 ± 6	51 ± 3	38 ± 6	35 ± 7	0
HuTipMab	82 ± 5	57 ± 6	57 ± 4	46 ± 8	41 ± 2	0
1:1 cocktail	**92 ± 1**	**79 ± 2**	**75 ± 3**	**61 ± 5**	42 ± 2	0
B. NTHI						
mB Box-97	62 ± 2	38 ± 11	32 ± 6	25 ± 7	15 ± 2	0
HuTipMab	67 ± 7	56 ± 3	41 ± 1	24 ± 14	13 ± 13	0
1:1 cocktail	**87 ± 0**	**79 ± 4**	**69 ± 5**	**57 ± 8**	**34 ± 7**	0
Key						
mB Box-97	900 nM	450 nM	225 nM	113 nM	56 nM	0 nM
HuTipMab	7.5 μg	3.8 μg	2.0 μg	1.0 μg	0.5 μg	0.00 μg

The relative percentage of (**A**) *S. aureus* or (**B**) NTHI biofilms prevented with exposure to 1:2 dilutions of single dose concentrations of mB Box-97_{syn}, HuTipMab, or a 1:1 cocktail of both agents (decreasing concentrations L→R) for 13 h for *S. aureus* or 16 h for NTHI. The 1:1 cocktail of each agent was more preventative than either agent used singly in all bolded cells. Data presented are mean percent biofilm biomass prevented compared to incubation with media alone ± SEM.

Table 1: **A cocktail of mB Box-97_{syn} and HuTipMab prevented biofilm formation in *vitro* as evaluated by CSLM with COMSTAT analysis of biofilm biomass.**

concentration that was approximately equally preventative to that percentage of biofilm growth prevented by HuTipMab when used singly. Exposure of NTHI to the same decreasing concentrations of a 1:1 cocktail (Panel B, bottommost row) yielded similar results (87%–0%) and notably exceeded that of either biological when used alone at every concentration tested.

mB Box-97_{syn} prevented aggregate biofilm formation and failed to induce an inflammatory response *in vivo*

To now determine whether mB Box-97_{syn} could also prevent aggregate biofilm formation *in vivo* and do so without promoting an excessive and potentially damaging inflammatory response, we used a murine model of aggregate biofilm formation in the lungs of mice wherein we have previously shown the ability of full length HMGB1 to promote clearance of aggregate *B. cenocepacia* biofilms from the lung.[14] To do so, we inoculated C57BL/6 mice with 10^7 colony forming units (CFU) of *B. cenocepacia*[14] and treated them with 2 μg of B Box-97 or mB Box-97_{syn} simultaneously at the time of intratracheal (i.t.) bacterial challenge. Animals were euthanised 72 h post challenge and CFU of bacteria within bronchoalveolar lavage (BAL) and lung homogenates were determined (Fig. 6A). Compared to untreated mice or mice treated with B Box-97, BAL of mice treated with mB Box-97_{syn} contained significantly fewer bacteria ($P = 0.02$). Although this significant difference was not observed in lung homogenates (Fig. 6B), there was nonetheless a trend for reduced CFU in the homogenates of the lungs of mice that received either B Box-97 or mB Box-97_{syn} compared to infected mice that received no treatment. Mouse lungs were also fixed, embedded in paraffin, sectioned then stained with hematoxylin and eosin (H&E) to assess relative signs of inflammation (Fig. 6C). Alveolar sacs and bronchial spaces of a representative uninfected mouse is shown (**a**) alongside that of an uninfected mouse treated with either B box-97 alone (**b**) or mB Box-97_{syn} alone (**c**), none of which exhibited signs of inflammation. Conversely however, the lungs of mice infected with *B. cenocepaicia* showed a profuse recruitment of inflammatory cells (**d**), mainly characterised by neutrophils distributed within alveolar sacs. The infected mice treated with either B Box-97 (**e**) or mB Box-97_{syn} (**f**) showed reduced recruitment of inflammatory cells, with very few PMNs present within the alveoli, particularly in the mB Box-97_{syn} treated mice. When found, the inflammatory cells were primarily observed surrounding the layer of airway epithelial cells that lined the bronchial spaces in infected mice treated with either B Box-97 or mB Box-97_{syn}. This outcome indicated that mB Box-97_{syn} not only limited the bacterial load within the lungs of challenged mice, but also did not induce a pro-inflammatory response compared to untreated/infected mice or those that had been infected but had also been treated with B Box-97.

To further demonstrate that neither B Box-97 nor mB Box-97_{syn} was proinflammatory, we utilised a murine model of systemic inflammation (or endotoxemia) wherein C57BL/6 mice were injected intraperitoneally (i.p.) with either *E. coli* lipopolysaccharide (LPS) or PBS as positive or negative controls, respectively or with 2 μg of B Box-97 or mB Box-97_{syn}. Twenty-four hours later, serum was collected and assayed for relative concentration of TNF-α (Fig. 7). Whereas LPS induced high levels of serum TNF-α, there was no similar outcome for mice injected with either PBS, B Box-97 or mB Box-$97_{syn.}$ These differences were statistically significant ($p \leq 0.0001$).

Discussion

Previously, we demonstrated full length HMGB1's anti-biofilm activity via its ability to act as a disruptive agent against a variety of Gram-negative and Gram-positive bacterial pathogens.[14] Herein we demonstrated that the truncated HMGB1 domains: B Box, A + B Boxes, mB Box-97, but not the A Box, disrupted biofilms formed by additional tested pathogens in a species agnostic manner. These data indicated that the domain variants of HMGB1 inclusive of the B Box domain were effective anti-biofilm agents. Furthermore, we extended our analysis to show that a naturally occurring cysteine that is, in part, responsible for HMGB1's proinflammatory activity can be mutated to a serine to be far less inflammatory in an animal model of a biofilm infection while its' DNA binding and anti-biofilm abilities were retained, which we demonstrated through use of the 97-mer polypeptide mB Box-97. Importantly, the aforementioned functions were retained even when mB Box-

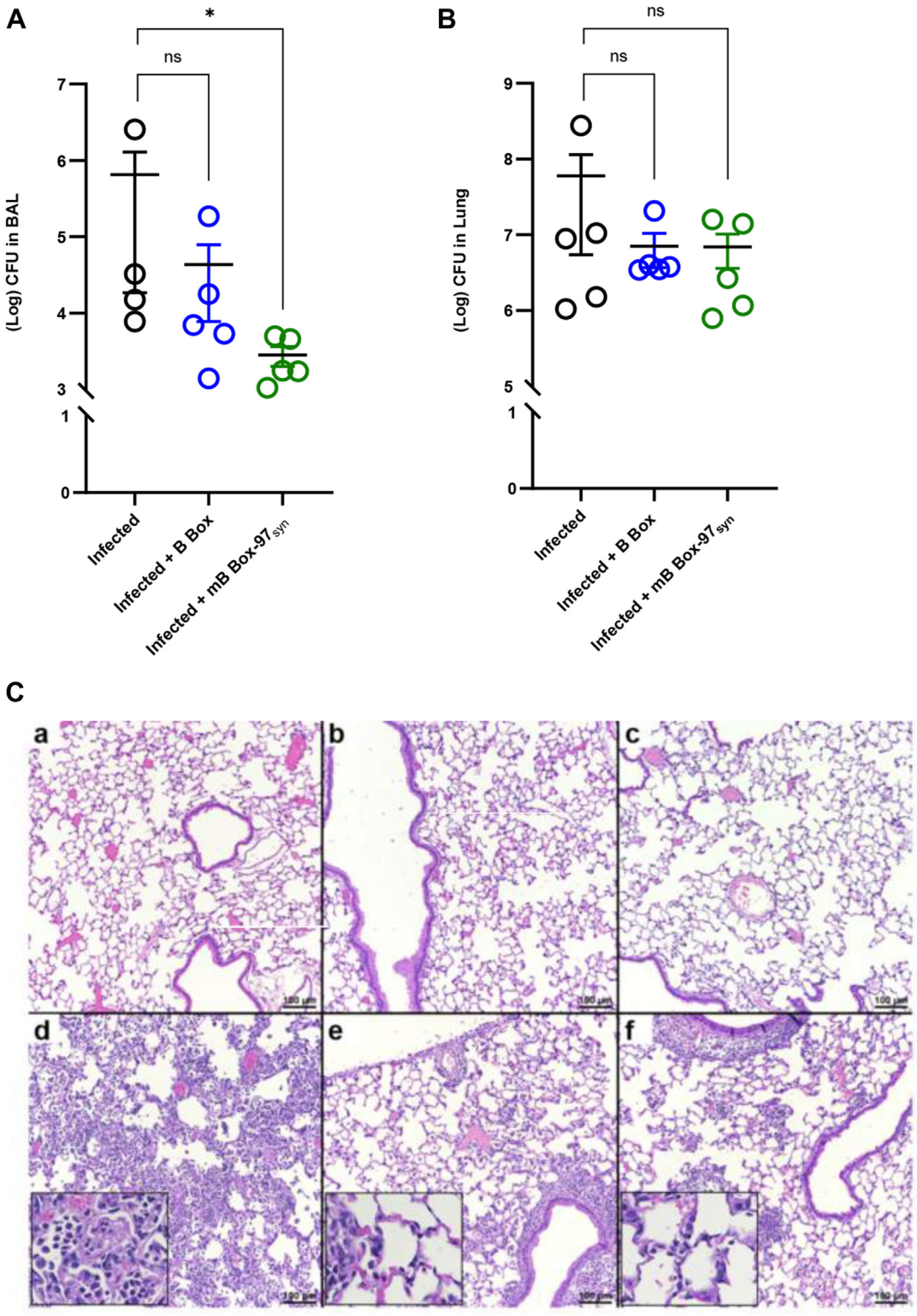

Fig. 6: **Prevention of *B. cenocepacia* aggregate biofilm formation in the murine lung without induction of excessive inflammation**. *C57BL/6* mice were infected IT with 10^7 CFU of *B. cenocepacia*. Mice were treated with 2 µg of B Box-97 or mB Box-97_{syn} peptides at the time of infection. Animals were euthanised 72 h post infection, and (**A**) bronchoalveolar lavage (BAL) or (**B**) lung tissue were collected (*P < 0.05).

97 was produced synthetically and devoid of post translational modifications (an indication that this domain is folded properly in the absence of any modification of cellular activities).

HMGB1 is among the most abundant, ubiquitous, and multifunctional eukaryotic cell proteins with context-dependent cellular functions.[32] Originally described as a nuclear non-histone protein whose biological roles appeared to require DNA binding,[33] further studies show that HMGB1 also functions outside of the cell where it exerts potent proinflammatory actions that can be considered DAMP mediators.[20,34,35] Additional studies show that HMGB1 plays a role in microbial elimination from the host, not only through its proinflammatory actions but also by the modulation of neutrophil chemotaxis and the induction of NET formation.[19,36,37]

HMGB1, a 25-kDa protein comprised of 215 amino acids, is organised into three functional domains: two net positively charged DNA-binding domains approximately 80 amino acids long, termed the A and B boxes that are connected by a short basic linker, and a negatively charged acidic C tail at the carboxyl-terminus that is comprised of 30 glutamic and aspartic acid residues. While the role of the C tail is largely elusive, it has been shown *in vitro* to regulate HMGB1 affinity for a variety of DNA structures.[37–40] TNF-stimulating activity of HMGB1 is localised within the B Box domain, and its immunogenic activity is altered when a cysteine at position 106 is mutated.[41] Specifically, the B Box domain of HMGB1 contains proinflammatory activity that relies on the presence of the C106-containing peptide. HMGB1's C106 residue is notably required for TLR4 binding and HMGB1-dependent cytokine release from macrophages. Through its ability to bind TLR4, HMGB1 triggers activation of a proinflammatory cascade that mediates tissue repair and wound regeneration. In the case of recalcitrant biofilm-mediated infections, however, the sustained activation of a proinflammatory cascade could be detrimental to the healing process, as excessive cytokine responses induced during infection could cause collateral damage to the host.[29] Herein, we introduced a modified truncation of HMGB1 inclusive of the HMGB1 B Box domain called mB Box-97, characterised by a mutation of residue C106 that virtually eliminated the proinflammatory ability of HMGB1, yet fully retained its biofilm eDNA binding plus biofilm disruptive and preventative capabilities.

eDNA is a crucial bacterial biofilm component which is maintained by the bacterial DNABII proteins (HU and IHF) localised to the vertices of crossed strands of eDNA that makes up the eDNA-dependent biofilm extracellular matrix.[12] Given that DNABII and HMGB1 proteins have similar DNA structure binding preferences *in vitro* that functionally can replace one another,[14,42] it was reasonable to conclude that HMGB1 could act at the same vertices of biofilm eDNA. Indeed, we recently discovered that HMGB1 acts as a competitive inhibitor of the DNABII proteins for the same eDNA binding sites thereby causing disruption of biofilms.[14] Our previous studies demonstrate that the vertices structure that we have shown functionally resemble HJs and are stabilised by the bacterial DNABII family of proteins have an essential role in the structural integrity of bacterial biofilms.[15] Indeed, both the DNABII family of proteins and HMGB1 bind to HJs.[43] However, there are important distinctions between these nucleoprotein interactions that contrast each protein's interaction with biofilm eDNA. First, HMGB1 and the DNABII family are non-homologous and share no known immunological epitopes. Second, HMGB1 and DNABII proteins bend DNA differently. HMGB1 binds to and bends via the convex side of DNA; in effect pushing the DNA into a bend, whereas the DNABII family binds to and bends via the concave side of DNA effectively pulling the DNA into a bent configuration.[44] Third, while both proteins bind to HJs, which is believed to be the consequence of HJ structure resembling bent DNA, the HMGB1 protein creates a square planar conformation of HJs, whereas the DNABII proteins create an X-like configuration.[45–47] The former allows branch migration of homologous strands of DNA, while the latter prevents branch migration. Whereas we do not know the exact structure of the HJ-like DNA configurations within biofilms, we noted previously that the DNABII proteins are found bound to the vertices (the HJ-like structures) of eDNA in biofilms, while HMGB1 is never found at these structures,[14] consistent with the notion that when HMGB1 encounters these structures, they are disrupted.

Given this model for biofilm disruption, we sought to identify which of HMGB1's DNA binding domains was responsible for biofilm disruption. In this work, we show that it is the B-box domain alone that is responsible for anti-biofilm activity. To validate that all of the constructs containing the B-Box were still able to bind DNA, we used HJ DNA as a proxy for the HJ-like structures in biofilms. Here, we determined that HMGB1 and its truncated variants retained their DNA-binding capabilities, a finding that supports our

(**C**) Lungs were fixed and embedded in paraffin; slides were stained with Hematoxylin-Eosin (H&E) and histopathology was evaluated. (a) uninfected lung; (b) lung from uninfected mouse treated with B Box-97; (c) lung from uninfected mouse treated with mB Box-97_{syn}; (d) lung from mouse challenged with *B. cenocepacia*; (e) lung from mouse challenged with *B. cenocepacia* and treated with B Box-97; (f) lung from mouse challenged with *B. cenocepacia* and treated with mB Box-97_{syn}. Images are shown at a magnification of 200x, the scale bar represents 100 μm. Insets within d, e & f are shown at a magnification of 600x.

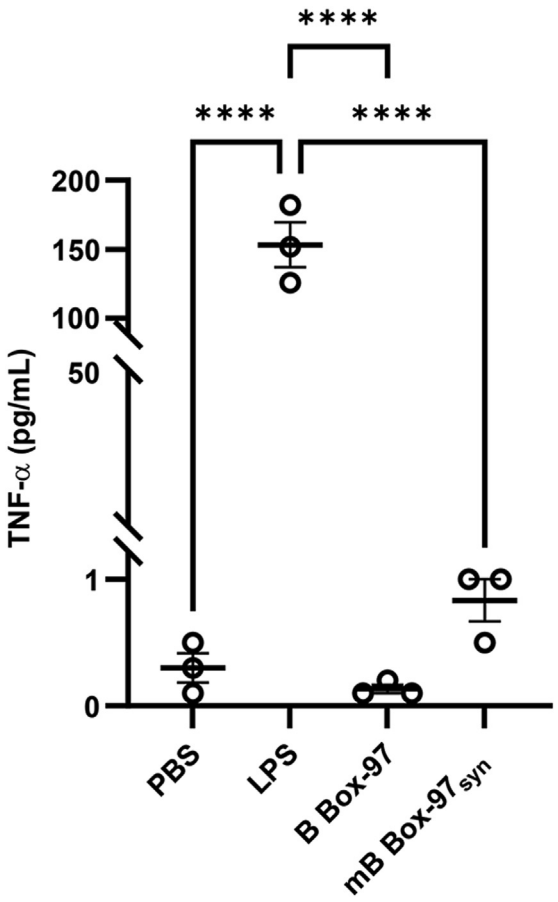

Fig. 7: **Neither B Box-97 nor mB Box-97_{syn} induced an inflammatory response in a murine model of endotoxemia** Mice were injected IP with either sterile PBS, 100 μg LPS, 2 μg endotoxin-free B Box-97, or 2 μg endotoxin-free mB Box-97_{syn}. Serum TNF-α was measured by ELISA after 24 h. Whereas LPS induced production of TNF-α, neither PBS, B Box-97 nor mB Box-97_{syn} induced formation of this pro-inflammatory cytokine. Bars represent mean ± SD.

hypothesis that the anti-biofilm activities of HMGB1 (and the structural variants) are mediated through DNA binding. Supportive of this hypothesis is the higher affinity to HJ DNA displayed by the B Box as compared to the A Box, where the latter consistently showed no anti-biofilm activity. Indeed, binding to and bending with high affinity to DNA with a preference for distorted (bent, kinked and unwound) DNA structures is an intrinsic feature of the HMGB1 Boxes.[39,40,48] However, the HMGB1 boxes have different preferences for four-way (HJ) DNA.[27,49] As shown in Fig. 1, the B Box-containing truncation we used in our experiments included an additional 8 amino acids (residues 80–176) beyond the canonical B Box domain that contains 4 positively charged amino acids (lysine) that are believed to facilitate DNA binding. This construction is similar to the longer B Box domain (residues (84–184) used by Teo et al.,[49] who tested the preferences of various HMGB1 Box domains for synthetic four–way junctions, the ability to bend DNA and found that the DNA/protein interactions and ability to bend DNA were weaker for A Box as compared with the B Box with the linker. They concluded that the additional B Box region (linker) might promote the recognition of protein/DNA complexes.[49,50] This finding is also in agreement with previous studies that describe the acidic C tail as lowering the affinity of A and B Boxes for DNA substrates.[38,51,52] This outcome can be a consequence of the interaction of the positively charged A and B Boxes with the negatively charged C terminal tail, as the two Boxes 'sandwich' the C tail so as the HMGB1 DNA-binding domains are shielded from interactions with DNA.[53,54] Likewise, removal of the C tail increased the affinity of the HMGB1 A and B Boxes with DNA.[54]

Our previous studies demonstrate that HMGB1 (and herein demonstrated that mB Box-97) binds the HJ-like structures responsible for maintaining structural integrity within biofilm eDNA matrices to destabilise them and likely function to cordon off and inhibit biofilm formation in the host. In contrast, anti-DNABII antibodies bind free DNABII proteins which introduces an equilibrium shift of DNABII proteins from the biofilm to subsequently collapse biofilm architecture.[14] Via their mechanistic differences, both strategies herein successfully disrupted and prevented biofilm formation. In this new study, we showed that mB Box-97_{syn} can be used in a combinatorial therapeutic approach to prevent or limit biofilm formation evidenced by use of a host-augmenting plus pathogen-directed anti-DNABII cocktail (mB Box-97_{syn} plus HuTipMab), which had biofilm prevention activity that exceeded preventative capabilities of either biological when used separately. A potential limitation of this study could be owed to use of static biofilms rather than biofilms grown under flow, whose extracellular matrices could indeed differ architecturally.

If this activity is maintained *in vivo*, we hypothesise that its therapeutic use would likely tip the therapeutic balance in favor of the host in both the prevention and likely eradication of highly recalcitrant bacterial biofilms. New work presented here shows that neither approach dominates the other and by acting via distinct mechanisms could constitute a complementary and highly powerful anti-biofilm disease therapeutic.

Toward the goal of clinical use, we created a version of HMGB1 that would retain anti-biofilm function but without proinflammatory activity by constructing a minimal B Box-containing peptide. Since HMGB1 functions as a proinflammatory innate immune effector[55] and when in excess can cause damaging inflammation, even to the point of sepsis, to do so we introduced a point mutation at C106S which is known to reduce inflammatory function.[29] Our fully functional anti-biofilm candidate mB Box-97_{syn} retains complete

anti-biofilm activity, but with the C106S mutation is no longer inflammatory. Indeed, our results indicated that mB Box-97$_{syn}$ fails to elicit the production of TNF-α as well as also facilitating a reduction of inflammatory infiltration to the lungs, without compromising bacterial clearance in an *in vivo* model of *B. cenocepacia* aggregate biofilm formation in the murine lung. Moreover, since this peptide is < 100 amino acids, it can be synthesised, and is devoid of mitigating activities derived from post translational modifications. Indeed, mB Box-97$_{rec}$ and mB Box97$_{syn}$ appear to be equivalent in their ability to act as anti-biofilm agents. Induced release of resident bacteria from a biofilm state into a free living yet highly antibiotic-vulnerable state[56–60] gives this new formulation clinical potential as a broad-spectrum anti-biofilm approach, which could be even further empowered with a co-delivered antibiotic depending on the specific disease state, site of disease and microbes within the biofilm.

Contributors

Conceptualisation: L.O.B., S.D.G.
Methodology: L.O.B., S.D.G., S.P.S., J.D.R., A.D., J.R.B, S.B., L.M.W., F.R.A.
Investigation: L.O.B., S.D.G., S.P.S., J.D.R., A.D., J.R.B, S.B., L.M.W, F.R.A.
Funding acquisition: L.O.B., S.D.G.
Supervision: L.O.B., S.D.G., S.P.S.
Writing—original draft: J.D.R, L.O.B., S.D.G.
Writing—review & editing: L.O.B., S.D.G., S.P.S., J.D.R., A.D., J.R.B., F.R.A., S.B., L.M.W.

Data sharing statement

The data that support the findings of this study are available from the corresponding authors upon reasonable request.

Declaration of interests

L.O.B. and S.D.G. are inventors of technology related to the DNABII directed approach, rights to which have been licensed to Clarametyx Biosciences, Inc., of which they are founders, shareholders, and members of the scientific advisory board. All other authors declare no conflict of interest.

Acknowledgements

We thank Jennifer Neelans for expert assistance with manuscript preparation. We are grateful to Parthiv Medidi who generated 48, 72, and 96 h NTHI biofilm disruption data (see Supplementary Figure S2). We thank the Biostatistics Resource at Nationwide Children's Hospital (BRANCH) for assistance with statistical analysis. This work was supported by NIH/NIDCD R01DC011818 to L.O.B. and S.D.G. and NIH/NIAID R01AI155501 to S.D.G.

Appendix A. Supplementary data

Supplementary data related to this article can be found at https://doi.org/10.1016/j.ebiom.2024.105304.

References

1 Agresti A, Scaffidi P, Riva A, Caiolfa VR, Bianchi ME. GR and HMGB1 interact only within chromatin and influence each other's residence time. *Mol Cell*. 2005;18(1):109–121. https://doi.org/10.1016/j.molcel.2005.03.005.
2 Mandke P, Vasquez KM. Interactions of high mobility group box protein 1 (HMGB1) with nucleic acids: implications in DNA repair and immune responses. *DNA Repair*. 2019;83:102701. https://doi.org/10.1016/j.dnarep.2019.102701.
3 Anggayasti WL, Mancera RL, Bottomley S, Helmerhorst E. The self-association of HMGB1 and its possible role in the binding to DNA and cell membrane receptors. *FEBS Lett*. 2017;591(2):282–294. https://doi.org/10.1002/1873-3468.12545.
4 Hoste E, Maueroder C, van Hove L, et al. Epithelial HMGB1 delays skin wound healing and drives tumor initiation by priming neutrophils for NET formation. *Cell Rep*. 2019;29(9):2689–2701.e4. https://doi.org/10.1016/j.celrep.2019.10.104.
5 Islam MM, Takeyama N. Role of neutrophil extracellular traps in health and disease pathophysiology: recent insights and advances. *Int J Mol Sci*. 2023;24(21):15805. https://doi.org/10.3390/ijms242115805.
6 Ceri H, Olson ME, Stremick C, Read RR, Morck D, Buret A. The Calgary Biofilm Device: new technology for rapid determination of antibiotic susceptibilities of bacterial biofilms. *J Clin Microbiol*. 1999;37(6):1771–1776. https://doi.org/10.1128/JCM.37.6.1771-1776.1999.
7 Frederiksen B, Pressler T, Hansen A, Koch C, Hoiby N. Effect of aerosolized rhDNase (Pulmozyme) on pulmonary colonization in patients with cystic fibrosis. *Acta Paediatr*. 2006;95(9):1070–1074. https://doi.org/10.1080/08035250600752466.
8 Whitchurch CB, Tolker-Nielsen T, Ragas PC, Mattick JS. Extracellular DNA required for bacterial biofilm formation. *Science*. 2002;295(5559):1487. https://doi.org/10.1126/science.295.5559.1487.
9 Kaplan JB, LoVetri K, Cardona ST, et al. Recombinant human DNase I decreases biofilm and increases antimicrobial susceptibility in staphylococci. *J Antibiot (Tokyo)*. 2012;65(2):73–77. https://doi.org/10.1038/ja.2011.113.
10 Koo H, Allan RN, Howlin RP, Stoodley P, Hall-Stoodley L. Targeting microbial biofilms: current and prospective therapeutic strategies. *Nat Rev Microbiol*. 2017;15(12):740–755. https://doi.org/10.1038/nrmicro.2017.99.
11 Buzzo JR, Devaraj A, Gloag ES, et al. Z-form extracellular DNA is a structural component of the bacterial biofilm matrix. *Cell*. 2021;184(23):5740–5758.e17. https://doi.org/10.1016/j.cell.2021.10.010.
12 Goodman SD, Obergfell KP, Jurcisek JA, et al. Biofilms can be dispersed by focusing the immune system on a common family of bacterial nucleoid-associated proteins. *Mucosal Immunol*. 2011;4(6):625–637. https://doi.org/10.1038/mi.2011.27.
13 Segall AM, Goodman SD, Nash HA. Architectural elements in nucleoprotein complexes: interchangeability of specific and non-specific DNA binding proteins. *EMBO J*. 1994;13(19):4536–4548. https://doi.org/10.1002/j.1460-2075.1994.tb06775.x.
14 Devaraj A, Novotny LA, Robledo-Avila FH, et al. The extracellular innate-immune effector HMGB1 limits pathogenic bacterial biofilm proliferation. *J Clin Invest*. 2021;131(16):e140527. https://doi.org/10.1172/JCI140527.
15 Devaraj A, Buzzo JR, Mashburn-Warren L, et al. The extracellular DNA lattice of bacterial biofilms is structurally related to Holliday junction recombination intermediates. *Proc Natl Acad Sci U S A*. 2019;116(50):25068–25077. https://doi.org/10.1073/pnas.1909017116.
16 Novotny LA, Goodman SD, Bakaletz LO. Targeting a bacterial DNABII protein with a chimeric peptide immunogen or humanised monoclonal antibody to prevent or treat recalcitrant biofilm-mediated infections. *eBioMedicine*. 2020;59:102867. https://doi.org/10.1016/j.ebiom.2020.102867.
17 Novotny LA, Jurcisek JA, Goodman SD, Bakaletz LO. Monoclonal antibodies against DNA-binding tips of DNABII proteins disrupt biofilms *in vitro* and induce bacterial clearance *in vivo*. *eBioMedicine*. 2016;10:33–44. https://doi.org/10.1016/j.ebiom.2016.06.022.
18 Brockson ME, Novotny LA, Mokrzan EM, et al. Evaluation of the kinetics and mechanism of action of anti-integration host factor-mediated disruption of bacterial biofilms. *Mol Microbiol*. 2014;93(6):1246–1258. https://doi.org/10.1111/mmi.12735.
19 Tadie JM, Bae HB, Jiang S, et al. HMGB1 promotes neutrophil extracellular trap formation through interactions with Toll-like receptor 4. *Am J Physiol Lung Cell Mol Physiol*. 2013;304(5):L342–L349. https://doi.org/10.1152/ajplung.00151.2012.
20 Wang H, Bloom O, Zhang M, et al. HMG-1 as a late mediator of endotoxin lethality in mice. *Science*. 1999;285(5425):248–251. https://doi.org/10.1126/science.285.5425.248.
21 Harrison A, Dyer DW, Gillaspy A, et al. Genomic sequence of an otitis media isolate of nontypeable *Haemophilus influenzae*: comparative study with *H. influenzae* serotype d, strain KW20. *J Bacteriol*. 2005;187(13):4627–4636. https://doi.org/10.1128/JB.187.13.4627-4636.2005.

22 Mulvey MA, Schilling JD, Hultgren SJ. Establishment of a persistent *Escherichia coli* reservoir during the acute phase of a bladder infection. *Infect Immun*. 2001;69(7):4572–4579. https://doi.org/10.1128/IAI.69.7.4572-4579.2001.

23 Abdulrahman BA, Khweek AA, Akhter A, et al. Autophagy stimulation by rapamycin suppresses lung inflammation and infection by *Burkholderia cenocepacia* in a model of cystic fibrosis. *Autophagy*. 2011;7(11):1359–1370. https://doi.org/10.4161/auto.7.11.17660.

24 Bhardwaj P, Ziegler E, Palmer KL. Chlorhexidine induces VanA-type vancomycin resistance genes in enterococci. *Antimicrob Agents Chemother*. 2016;60(4):2209–2221. https://doi.org/10.1128/AAC.02595-15.

25 Storm DW, Koff SA, Horvath DJ Jr, Li B, Justice SS. *In vitro* analysis of the bactericidal activity of *Escherichia coli* Nissle 1917 against pediatric uropathogens. *J Urol*. 2011;186(4 Suppl):1678–1683. https://doi.org/10.1016/j.juro.2011.04.021.

26 Muller S, Ronfani L, Bianchi ME. Regulated expression and subcellular localization of HMGB1, a chromatin protein with a cytokine function. *J Intern Med*. 2004;255(3):332–343. https://doi.org/10.1111/j.1365-2796.2003.01296.x.

27 Bianchi ME, Beltrame M, Paonessa G. Specific recognition of cruciform DNA by nuclear protein HMG1. *Science*. 1989;243(4894 Pt 1):1056–1059. https://doi.org/10.1126/science.2922595.

28 Starkova TY, Polyanichko AM, Artamonova TO, Tsimokha AS, Tomilin AN, Chikhirzhina EV. Structural characteristics of high-mobility group proteins HMGB1 and HMGB2 and their interaction with DNA. *Int J Mol Sci*. 2023;24(4):3577. https://doi.org/10.3390/ijms24043577.

29 Yang H, Hreggvidsdottir HS, Palmblad K, et al. A critical cysteine is required for HMGB1 binding to Toll-like receptor 4 and activation of macrophage cytokine release. *Proc Natl Acad Sci U S A*. 2010;107(26):11942–11947. https://doi.org/10.1073/pnas.1003893107.

30 Heydorn A, Nielsen AT, Hentzer M, et al. Quantification of biofilm structures by the novel computer program COMSTAT. *Microbiology (Read)*. 2000;146(Pt 10):2395–2407. https://doi.org/10.1099/00221287-146-10-2395.

31 Yang H, Lundback P, Ottosson L, et al. Redox modifications of cysteine residues regulate the cytokine activity of HMGB1. *Mol Med*. 2021;27(1):58. https://doi.org/10.1186/s10020-021-00307-1.

32 Tang D, Kang R, Zeh HJ, Lotze MT. The multifunctional protein HMGB1: 50 years of discovery. *Nat Rev Immunol*. 2023;23(12):824–841. https://doi.org/10.1038/s41577-023-00894-6.

33 Goodwin GH, Johns EW. Isolation and characterisation of two calf-thymus chromatin non-histone proteins with high contents of acidic and basic amino acids. *Eur J Biochem*. 1973;40(1):215–219. https://doi.org/10.1111/j.1432-1033.1973.tb03188.x.

34 Berthelot F, Fattoum L, Casulli S, Gozlan J, Marechal V, Elbim C. The effect of HMGB1, a damage-associated molecular pattern molecule, on polymorphonuclear neutrophil migration depends on its concentration. *J Innate Immun*. 2012;4(1):41–58. https://doi.org/10.1159/000328798.

35 Scaffidi P, Misteli T, Bianchi ME. Release of chromatin protein HMGB1 by necrotic cells triggers inflammation. *Nature*. 2002;418(6894):191–195. https://doi.org/10.1038/nature00858.

36 Peng HH, Liu YJ, Ojcius DM, et al. Mineral particles stimulate innate immunity through neutrophil extracellular traps containing HMGB1. *Sci Rep*. 2017;7(1):16628. https://doi.org/10.1038/s41598-017-16778-4.

37 Andersson U, Tracey KJ. HMGB1 is a therapeutic target for sterile inflammation and infection. *Annu Rev Immunol*. 2011;29:139–162. https://doi.org/10.1146/annurev-immunol-030409-101323.

38 Blair RH, Horn AE, Pazhani Y, Grado L, Goodrich JA, Kugel JF. The HMGB1 C-terminal tail regulates DNA bending. *J Mol Biol*. 2016;428(20):4060–4072. https://doi.org/10.1016/j.jmb.2016.08.018.

39 Stros M. HMGB proteins: interactions with DNA and chromatin. *Biochim Biophys Acta*. 2010;1799(1-2):101–113. https://doi.org/10.1016/j.bbagrm.2009.09.008.

40 Thomas JO, Travers AA. HMG1 and 2, and related 'architectural' DNA-binding proteins. *Trends Biochem Sci*. 2001;26(3):167–174. https://doi.org/10.1016/s0968-0004(01)01801-1.

41 Kazama H, Ricci JE, Herndon JM, Hoppe G, Green DR, Ferguson TA. Induction of immunological tolerance by apoptotic cells requires caspase-dependent oxidation of high-mobility group box-1 protein. *Immunity*. 2008;29(1):21–32. https://doi.org/10.1016/j.immuni.2008.05.013.

42 Goodman SD, Nicholson SC, Nash HA. Deformation of DNA during site-specific recombination of bacteriophage lambda: replacement of IHF protein by HU protein or sequence-directed bends. *Proc Natl Acad Sci U S A*. 1992;89(24):11910–11914. https://doi.org/10.1073/pnas.89.24.11910.

43 Pontiggia A, Negri A, Beltrame M, Bianchi ME. Protein HU binds specifically to kinked DNA. *Mol Microbiol*. 1993;7(3):343–350. https://doi.org/10.1111/j.1365-2958.1993.tb01126.x.

44 Rice PA, Yang S, Mizuuchi K, Nash HA. Crystal structure of an IHF-DNA complex: a protein-induced DNA U-turn. *Cell*. 1996;87(7):1295–1306. https://doi.org/10.1016/s0092-8674(00)81824-3.

45 Bonnefoy E, Takahashi M, Yaniv JR. DNA-binding parameters of the HU protein of Escherichia coli to cruciform DNA. *J Mol Biol*. 1994;242(2):116–129. https://doi.org/10.1006/jmbi.1994.1563.

46 Vitoc CI, Mukerji I. HU binding to a DNA four-way junction probed by Forster resonance energy transfer. *Biochemistry*. 2011;50(9):1432–1441. https://doi.org/10.1021/bi1007589.

47 Pohler JR, Norman DG, Bramham J, Bianchi ME, Lilley DM. HMG box proteins bind to four-way DNA junctions in their open conformation. *EMBO J*. 1998;17(3):817–826. https://doi.org/10.1093/emboj/17.3.817.

48 Stros M, Launholt D, Grasser KD. The HMG-box: a versatile protein domain occurring in a wide variety of DNA-binding proteins. *Cell Mol Life Sci*. 2007;64(19-20):2590–2606. https://doi.org/10.1007/s00018-007-7162-3.

49 Teo SH, Grasser KD, Thomas JO. Differences in the DNA-binding properties of the HMG-box domains of HMG1 and the sex-determining factor SRY. *Eur J Biochem*. 1995;230(3):943–950. https://doi.org/10.1111/j.1432-1033.1995.tb20640.x.

50 Hardman CH, Broadhurst RW, Raine AR, Grasser KD, Thomas JO, Laue ED. Structure of the A-domain of HMG1 and its interaction with DNA as studied by heteronuclear three- and four-dimensional NMR spectroscopy. *Biochemistry*. 1995;34(51):16596–16607. https://doi.org/10.1021/bi00051a007.

51 Ueda T, Chou H, Kawase T, Shirakawa H, Yoshida M. Acidic C-tail of HMGB1 is required for its target binding to nucleosome linker DNA and transcription stimulation. *Biochemistry*. 2004;43(30):9901–9908. https://doi.org/10.1021/bi035975l.

52 Muller S, Bianchi ME, Knapp S. Thermodynamics of HMGB1 interaction with duplex DNA. *Biochemistry*. 2001;40(34):10254–10261. https://doi.org/10.1021/bi0100900.

53 Knapp S, Muller S, Digilio G, Bonaldi T, Bianchi ME, Musco G. The long acidic tail of high mobility group box 1 (HMGB1) protein forms an extended and flexible structure that interacts with specific residues within and between the HMG boxes. *Biochemistry*. 2004;43(38):11992–11997. https://doi.org/10.1021/bi049364k.

54 Stott K, Watson M, Howe FS, Grossmann JG, Thomas JO. Tail-mediated collapse of HMGB1 is dynamic and occurs via differential binding of the acidic tail to the A and B domains. *J Mol Biol*. 2010;403(5):706–722. https://doi.org/10.1016/j.jmb.2010.07.045.

55 Kang R, Chen R, Zhang Q, et al. HMGB1 in health and disease. *Mol Aspects Med*. 2014;40:1–116. https://doi.org/10.1016/j.mam.2014.05.001.

56 Wilbanks KQ, Mokrzan EM, Kesler TM, Kurbatfinski N, Goodman SD, Bakaletz LO. Nontypeable *Haemophilus influenzae* released from biofilm residence by monoclonal antibody directed against a biofilm matrix component display a vulnerable phenotype. *Sci Rep*. 2023;13(1):12959. https://doi.org/10.1038/s41598-023-40284-5.

57 Petrova OE, Sauer K. Escaping the biofilm in more than one way: desorption, detachment or dispersion. *Curr Opin Microbiol*. 2016;30:67–78. https://doi.org/10.1016/j.mib.2016.01.004.

58 Chambers JR, Cherny KE, Sauer K. Susceptibility of *Pseudomonas aeruginosa* dispersed cells to antimicrobial agents is dependent on the dispersion cue and class of the antimicrobial agent used. *Antimicrob Agents Chemother*. 2017;61(12):e00846–e00917. https://doi.org/10.1128/AAC.00846-17.

59 Goodwine J, Gil J, Doiron A, et al. Pyruvate-depleting conditions induce biofilm dispersion and enhance the efficacy of antibiotics in killing biofilms *in vitro* and *in vivo*. *Sci Rep*. 2019;9(1):3763. https://doi.org/10.1038/s41598-019-40378-z.

60 Zemke AC, D'Amico EJ, Snell EC, Torres AM, Kasturiarachi N, Bomberger JM. Dispersal of epithelium-associated *Pseudomonas aeruginosa* biofilms. *mSphere*. 2020;5(4):e00630–e00720. https://doi.org/10.1128/mSphere.00630-20.